Scanning Force Microscopy Studies on Molecular Packing and Friction Anisotropy in Thin Films of Tetranitrotetrapropoxycalix[4]arene

Holger Schönherr,[†] Paul J. A. Kenis,[‡] Johan F. J. Engbersen,[‡] Sybolt Harkema,[§] Ron Hulst,[∥] David N. Reinhoudt,*[,‡] and G. Julius Vancso*[,†]

Faculty of Chemical Technology, University of Twente, P.O. Box 217, 7500 AE Enschede, The Netherlands

Received November 3, 1997. In Final Form: February 19, 1998

Thin films of tetranitrotetrapropoxycalix[4]arene (**1**) show an unusual phase behavior and the formation of a complex multidomain structure. An endothermic phase transition, which occurs between 130 and 140 °C in bulk, was studied using differential scanning calorimetry, optical microscopy, magic angle solid-state NMR, and X-ray crystallography. In annealed films of **1**, two types of crystalline domains (I and II) can be distinguished with different optical, morphological, and friction properties. These domains were investigated at the molecular level by a combination of multimode scanning force microscopy (SFM), optical microscopy, and X-ray diffraction experiments. SFM force measurements as well as tapping mode phase images showed that different functional groups are exposed at the surface for the different domains. The friction forces observed in SFM depend on the type of domain, the applied load, and the orientation of the domain with respect to the scanning direction. The friction forces observed at normal forces below ca. 240 nN are lower for type I domains than for type II domains. For forces higher than 260 nN an *inversion of the relative friction* is observed. Moreover, type I domains exhibit a *friction anisotropy* that can be attributed to different orientations of the molecular crystal structure with respect to the scanning direction. Two lattices were observed by high-resolution SFM in type I domains, one of rectangular symmetry (x = 10.0 Å, y = 11.8 Å, α = 90°) and one of pseudohexagonal symmetry (d = 11.6 Å), which were in agreement with the parameters of the (010) and (011) facets of the X-ray single-crystal structure (a = 23.94 Å, b = 33.01 Å, c = 20.59 Å, and α, β, γ = 90°). In conclusion, the molecular packing and friction properties of the multidomain structure of thin films of **1** could be elucidated by SFM and complementary methods.

Introduction

Synthetic routes for selective functionalization of calix[4]arenes[1] are nowadays well developed. Control of the spatial orientation of functional groups in these molecules opens up the possibility for practical applications. Functionalized calix[4]arene molecules have been applied in various areas including sensors,[2] molecular recognition,[3] and molecular switches.[4] Previously, we showed that tetranitrotetrapropoxycalix[4]arene (**1**) (Chart 1), combining four donor−π-acceptor chromophoric units in one molecule, has interesting nonlinear optical properties.[5−7] In this paper we report on our studies of the material properties of neat **1** in the solid phase and in thin films. The typical phase transition of solid **1** at temperatures between 130 and 140 °C was investigated in detail. The surface structure of the annealed solid films of tetranitrotetrapropoxycalix[4]arene (**1**) was characterized by scanning force microscopy (SFM), optical microscopy, differential scanning calorimetry (DSC) and thin film X-ray diffraction. In addition, the anisotropic frictional properties of these films as studied by SFM (lateral force microscopy) are described.

Chart 1. Structure of Tetranitrotetrapropoxycalix[4]arene (1)

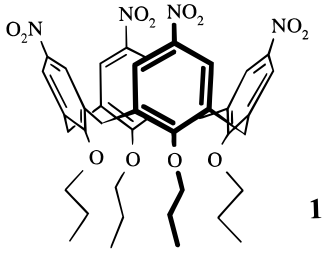

1

SFM and related scanning probe techniques provide valuable information about the surface on a scale of 100

* To whom correspondence should be addressed. Tel.: ++31 53 489 2967. Fax: ++31 53 489 3823. E-mail: g.j.vancso@ct.utwente.nl.

[†] Department of Polymer Materials Science and Technology.

[‡] Department of Supramolecular Chemistry and Technology/ MESA Research Institute.

[§] Chemical Physics Laboratory.

[∥] Laboratory of Chemical Analysis.

(1) For a recent review on calix[4]arenes see: Böhmer, V. *Angew. Chem., Int. Ed. Engl.* **1995**, *34*, 713.

(2) (a) Cobben, P. L. H. M.; Egberink, R. J. M.; Bomer, J. G.; Bergveld, P.; Reinhoudt, D. N. *J. Am. Chem. Soc.* **1992**, *114*, 10573. (b) Lugtenberg, R. J. W.; Antonisse, M. M. G.; Egberink, R. J. M.; Engbersen, J. F. J.; Reinhoudt, D. N. *J. Chem. Soc., Perkin Trans. 2* **1996**, 1937. (c) Kimura, K.; Tsujimura, Y.; Yokoyama, M. *Pure Appl. Chem.* **1995**, 67, 1085.

(3) Linnane, P.; James, T. D.; Shinkai, S. *J. Chem. Soc., Chem. Commun.* **1995**, 1997.

(4) (a) Timmerman, P.; Nierop, K. G. A.; Brinks, E. A.; Verboom, W.; van Veggel, F. C. J. M.; van Hoorn, W. P.; Reinhoudt, D. N. *Chem. Eur. J.* **1995**, *1*, 124. (b) Timmerman, P.; Verboom, W.; van Veggel, F. C. J. M.; van Duynhoven; J. P. M.; Reinhoudt, D. N. *Angew. Chem., Int. Ed. Engl.* **1994**, *33*, 2345.

(5) (a) Kelderman, E.; Heesink, G. J. T.; Derhaeg, L.; Verbiest, T.; Klaase, P. T. A.; Verboom, W.; Engbersen, J. F. J.; van Hulst, N. F.; Persoons, A.; Reinhoudt, D. N. *Angew. Chem., Int. Ed. Engl.* **1992**, *31*, 1074. (b) Kelderman, E.; Derhaeg, L.; Heesink, G. J. T.; Verboom, W.; Engbersen, J. F. J.; van Hulst, N. F.; Clays, K.; Persoons, A.; Reinhoudt, D. N. *Adv. Mater.* **1993**, *5*, 925. (c) Kenis, P. J. A.; Noordman, O. F. J.; van Hulst, N. F.; Engbersen, J. F. J.; Reinhoudt, D. N.; Hams, B. H. M.; van der Vorst, C. P. J. M. *Chem. Mater.* **1997**, *9*, 596.

(6) (a) Noordman, O. F. J.; van Hulst, N. F.; Bölger, B. *J. Opt. Soc. Am. B* **1995**, *12*, 2398. (b) Kenis, P. J. A.; Noordman, O. F. J.; Engbersen, J. F. J.; van Hulst, N. F.; Reinhoudt, D. N. *Polym. Mater. Sci. Eng.* **1996**, *75*, 317.

(7) Kenis, P. J. A.; Noordman, O. F. J.; Schönherr, H.; Kerver, E. G.; Snellink-Ruël, B. H. M.; van Hummel, H. J.; Harkema, S.; van der Vorst, C. P. J. M.; Hare, J.; Picken, S.; Engbersen, J. F. J.; Vancso, G. J.; van Hulst, N. F.; Reinhoudt, D. N. *Chem. Eur. J.*, in press.

S0743-7463(97)01198-0 CCC: $15.00 © 1998 American Chemical Society
Published on Web 04/21/1998

μm to 10 nm,[8] and in some cases even on the molecular level. The information extracted from different techniques with different contrast mechanisms in SFM can include details of topography (height information), friction (lateral force microscopy, LFM), attractive or repulsive forces, and local viscoelastic properties of the material of interest.[8]

SFM has become one of the methods of choice to investigate the surface structure in thin, molecularly organized films. Recently, we reported on the characterization of self-assembled monolayers of calix[4]-resorcinarene dialkyl-thioether derivatives on gold(111) by SFM.[9] Chi et al. used SFM to differentiate between different domains of Langmuir−Blodgett (LB) films based on the difference in the viscoelastic response.[10]

The frictional properties of inhomogeneous surfaces can be studied by SFM from micrometer to nanometer scales. Such "nano-tribology" studies often showed surprising results. For example, Last and Ward observed a friction anisotropy in unannealed and partially annealed epitaxial molecular films of bis(ethylenedithiolo)tetrathiofulvalene.[11] Until recently, only a limited number of examples of anisotropic friction on the nanometer scale had been reported, but friction anisotropy is not expected to be restricted to specific materials. It has been observed for various materials with oriented surface structures such as highly oriented pyrolytic graphite,[12] lipid bilayers,[13] polymer single crystals,[14] poly(tetrafluoroethylene),[15,16] polyethylene,[16] and transcrystallized poly(ethylene oxide).[17] The origin of friction anisotropy in these samples is in all cases due to the different azimuthal orientation of structurally equivalent domains or features. The domains can consist of crystal lattices,[11−13,15,16] polymer single-crystal fold planes[14] or lamellar polymer crystals.[17]

Experimental Section

General Information. Tetranitrotetrapropoxycalix[4]arene was synthesized as described earlier.[7,18] Films were prepared in a clean room facility (dust class 100 and 50% relative humidity) by spin-coating of a chloroform solution of tetranitrotetrapropoxycalix[4]arene (**1**) on cleaned (rinsing with superdistilled water and acetone, p.a., respectively) Pyrex glass (2 s at 200 rpm, >40 s at 1600 rpm). Films were obtained with thicknesses in the range of 190−210 nm, as determined with a Sloan Dektak 3030. After spin-coating, the films were annealed on a hot stage at 150 °C for at least 3 min. The domain structure was not affected by repeated heating and cooling cycles unless the samples were heated for a long time at 150 °C.

For *optical microscopy* an Olympus microscope BH2-UMA, equipped with an C35AD-4 camera was used. *DSC experiments* were performed on a Perkin-Elmer DSC7 calorimeter with heating rates of 20 or 30 °C/min. The *solid-state NMR experiments* were performed on a Varian Unity 400WB NMR spectrometer operating at 100 MHz for the ^{13}C atoms, equipped with a Jakobsen-design probehead in combination with a Sörensen heating unit and a Varian rotor speed control unit. The 5 mm ZrO_2 spinners were spun at the magic angle with a speed of 4 kHz.

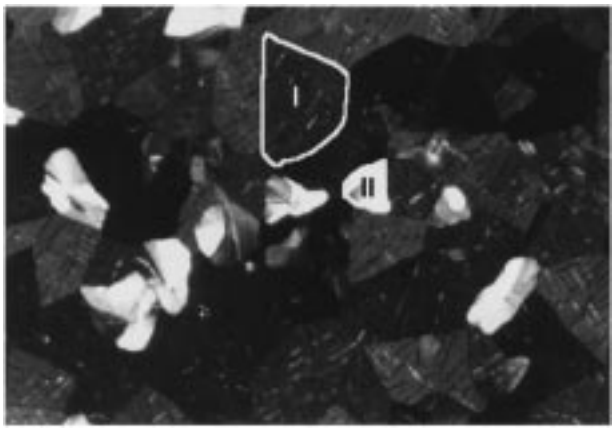

Figure 1. Optical microscopy of spin-coated tetranitrotetrapropoxycalix[4]arene films annealed at 150 °C (crossed polarizers, 160 × 110 μm^2). Type I and type II domains are indicated.

To visualize the different facets of the *X-ray structure* of **1**, a Cerius$^{\#2}$ software package of Biosym/Molecular Simulations was used.[19]

The specular angle *X-ray diffraction* measurements *on the films* were performed on a Philips X-ray powder diffractometer (cobalt source, λ = 1.7903 Å, angle of incidence θ (10−30°)).

Scanning Force Microscopy. The measurements were carried out with a NanoScope II and a NanoScope III multimode SFM from Digital Instruments (DI), Santa Barbara, CA. Contact mode SFM scans (NanoScope II and III) were performed both in air, utilizing cantilevers with a nominal spring constant of 0.38 N/m (Si_3N_4, DI), and in water (Millipore), utilizing a liquid cell (DI) and cantilevers with a nominal spring constant of 0.12 N/m (Si_3N_4, DI). Tapping mode SFM experiments (NanoScope III) were performed in air with silicon cantilevers (cantilever resonance frequency f_o = 280−320 kHz, DI). The instrument was operated at a slightly lower frequency than the natural resonance frequency. The tapping amplitude was set to 5.0−6.0 V; the setpoint ratio was chosen between 0.90 and 0.95.

All images shown in this work correspond to raw data that were plane-fitted. For high resolution, the SFM scan assembly with the sample mounted was allowed to equilibrate for 24 h prior to measurements in air. Digital filtering was used to eliminate noise (high-pass set to 4, low-pass set to 1). The lattice periodicities were observed both with and without these filters. The procedure used to obtain the lattice constants and lattice symmetry was described previously.[9] The calculated averages are stated together with the standard deviation. For the quantitative evaluation of the friction force micrographs the software "NIH image" was used.[11] The *z*-heights of all pixels of a chosen domain were plotted as histograms. The average value normalized by the value for one type Ib domain was used to estimate the friction contrast. The force measurements were performed under water (Millipore) at more than five different locations of a domain. The values of the pull-off (or pull-out) force of individual force distance curves were plotted as histograms and the average pull-out force was calculated.[20]

Results and Discussion

Phase Behavior. *Optical microscopy* of spin-coated, non-annealed films of tetranitrotetrapropoxycalix[4]arene (**1**) with crossed polarizers showed no birefringence. However, after annealing at 150 °C for at least 3 min, two types of birefringent domains with sizes up to 1600 μm^2 could be distinguished (Figure 1). This observation is

(8) For a recent review see: Magonov, S. N.; Whangbo, M. H. *Surface Analysis with STM and AFM*; VCH: Weinheim, 1996.
(9) Schönherr, H.; Vancso, G. J.; Huisman, B.-H.; van Veggel, F. C. J. M.; Reinhoudt, D. N. *Langmuir* **1997**, *13*, 1567.
(10) Chi, L.-F.; Anders, M.; Fuchs, H.; Johnston, R. R.; Ringsdorf, H. *Science* **1993**, *259*, 213.
(11) Last, J. A.; Ward, M. D. *Adv. Mater.* **1996**, *8*, 730.
(12) Mate, C. M.; McCelland, G. M.; Erlandsson, R.; Chiang, S. *Phys. Rev. Lett.* **1987**, *59*, 1942.
(13) Overney, R. M.; Takano, H.; Fujihira, M.; Paulus, W.; Ringsdorf, H. *Phys. Rev. Lett.* **1994**, *72*, 3546.
(14) (a) Nisman, R.; Smith, P.; Vancso, G. J. *Langmuir* **1994**, *10*, 1667. (b) Smith, P. F.; Nisman, R.; Ng, C.; Vancso, G. J. *Polym. Bull.* **1994**, *33*, 459.
(15) Vancso, G. J.; Förster, S.; Leist, H. *Macromolecules* **1996**, *29*, 2158.
(16) Schönherr, H.; Vancso, G. J. *Macromolecules* **1997**, *30*, 6391.
(17) Schönherr, H.; Vancso, G. J. *Polym. Prepr.*, in press.
(18) Verboom, W.; Durie, A.; Egberink, R. J. M.; Asfari, Z.; Reinhoudt, D. N. *J. Org. Chem.* **1992**, *57*, 1313.
(19) Cerius$^{\#2}$ Molecular Modeling Software for Materials Research from BIOSYM/Molecular Simulations Inc. San Diego, CA, and Cambridge, U.K.
(20) Schönherr, H.; Vancso, G. J. *Polym. Prepr.* **1996**, *37*, 612.

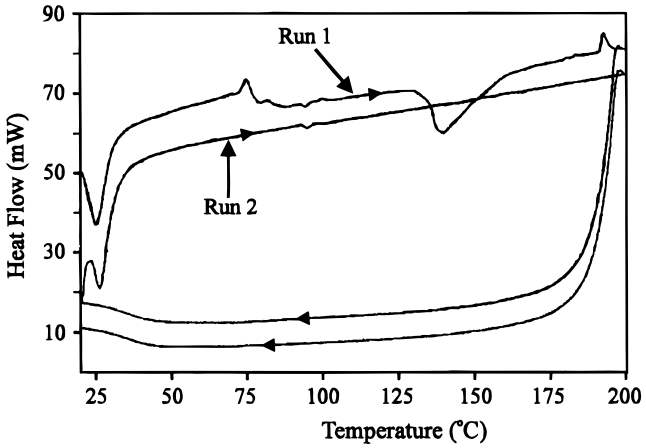

Figure 2. Differential scanning calorimetric runs of tetranitrotetrapropoxycalix[4]arene **1**.

evidence for a phase transition that takes place during annealing. Depending on the orientation of the domains with respect to the polarizers, the type I domains appear as light to dark gray areas, whereas type II domains appear as either completely dark or transparent areas. Thus, the orientation of the optical axes in the two domains is different. Also, the morphology of the two domains is significantly different as type I shows parallel stripes, and type II exhibits radiating features.

The *phase behavior* of tetranitrotetrapropoxycalix[4]-arene (**1**) was studied in more detail by differential scanning calorimetry (DSC), optical microscopy, magic angle solid-state NMR, and X-ray crystallography. In Figure 2 the traces of two subsequent *differential scanning calorimetry* runs of a microcrystalline sample of calix[4]-arene **1** are shown. An endothermic phase transition between 130 and 140 °C is observed during the first heating. The absence of this phase transition in the second run after cooling at a rate of 20 °C/min indicates the occurrence of an irreversible phase transition during the first run.[21] Initially, no birefringence was observed for a film of **1** by *polarization microscopy* upon heating from room temperature to 140 °C (10 °C/min). However, at 140 °C several birefringent domains started to grow. Eventually, the same ordered, birefringent structure was observed as for the films that were annealed at 150 °C for 15 min. This birefringent domain structure remained unchanged after cooling to room temperature.

Solid state ^{13}C NMR spectra (CP-MAS) of a microcrystalline sample of **1** were recorded at temperatures below and above the phase transition temperature, to gain more information about the symmetry of the thermodynamically stable phase obtained after heating (Figure 3). The narrow line width in all spectra confirms the crystalline nature of both phases of the material. For a calix[4]arene in a pinched cone conformation, two resonances are expected for each carbon atom in the solid state due to its C_{2v} symmetry, except for the methylene groups that connect the arene units. This pattern is observed for the phase that is present before the phase transition occurs (Figure 3a,b). The occurrence of the phase transition between 100 and 150 °C (Figure 3b,c, respectively) can be clearly deduced from the doubling of most of the signals. Since the spectrum does not change upon cooling (Figure 3c,d) it is evident that the phase transition is irreversible, in agreement with the results of the DSC and optical microscopy measurements described above. The doubling of the resonances implies that in the thermodynamically more stable crystalline phase, which results from annealing, two different types of calix[4]arenes in the pinched cone conformation are present. The fact that the $T_1\rho$ times (lattice relaxation times, not shown) of the resonances belonging to the different pinched cone conformations are similar indicates that these two calix[4]arene molecules are probably located within one asymmetric unit. However, based on this data it is difficult to assign the observed sets of resonances to certain structures, as chemical shifts in solid state NMR depend not only on the molecular structure but also on the packing of the molecules in the lattice.

Powder X-ray diffraction confirmed that, upon heating of the polycrystalline material **1**, a different crystalline phase is obtained.[22] Whereas non-annealed films of **1** show no diffraction peaks in *X-ray diffraction*, indicating an amorphous structure, a single diffraction peak was observed for annealed films of **1** at an angle corresponding to a lattice constant of 8.92 ± 0.05 Å. This clearly indicates the crystalline character of the annealed films.[23]

In conclusion, the results of DSC, optical microscopy, solid-state ^{13}C NMR and X-ray diffraction on films of **1** show that, after spin-coating, an amorphous phase is obtained, which is transferred into a thermodynamically more stable crystalline phase upon annealing above 140 °C.

Scanning Force Microscopy. As shown in the polarization microscopy picture (Figure 1), the crystalline surfaces of the annealed films show two different types of domains. These domain structures were investigated by multimode SFM. Parts a and b of Figure 4 display contact and tapping mode SFM micrographs of different locations of the same specimen. The features of the observed morphologies in the optical micrographs (Figure 1) can also be observed in the corresponding SFM height images (Figure 4a,b, left). Type I domains possess almost parallel cracks or depressions, whereas type II domains can be distinguished due to their radiating features.

Friction Properties. Friction force micrographs of annealed films of **1** exhibit clear differences between the two types of domains; see, e.g., Figure 4a. The friction with a silicon nitride tip on domain II was higher than that on domain I. The contrast in the friction image is *not* related to the topography. This can be concluded from the inversion of the friction contrast observed on flat areas of the sample when the data points were collected by scanning from right to left (retrace) instead of left to right (trace).[24] In the tapping mode phase images, the different domains could also be identified (Figure 4b). A phase shift is observed for type II domains, relative to type I domains, which is indicative of differences in adhesion forces.[25]

The differences in friction between the two domains can either be caused by the presence of different crystal

(21) The phase transition was absent after storage of the sample for 2 months, which additionally proves its irreversibility. In accordance with this is the observation of the same phase transition in DSC of samples of unheated films, whereas no phase transition is observed for annealed films (150 °C). These samples are prepared by scratching of the material from the glass substrate with a scalpel knife.

(22) The formation of a different crystal structure is evident from the dramatic change of the reflections upon passing through 140 °C. However, in the powder X-ray diffraction spectrum, the number of diffractions was too small to determine the unit cell of the crystalline phase obtained after annealing.

(23) Unfortunately, the films were too thin to solve the structure by a single-crystal crystallography. Furthermore, film preparation via the melt is not possible because of decomposition above the melting point (310 °C).

(24) The effect of the topography can be seen in domain I (Figure 4a). This can be observed in general when surfaces with edges are imaged.

(25) Tamayo, J.; Garcia, R. *Langmuir* **1996**, *12*, 4430.

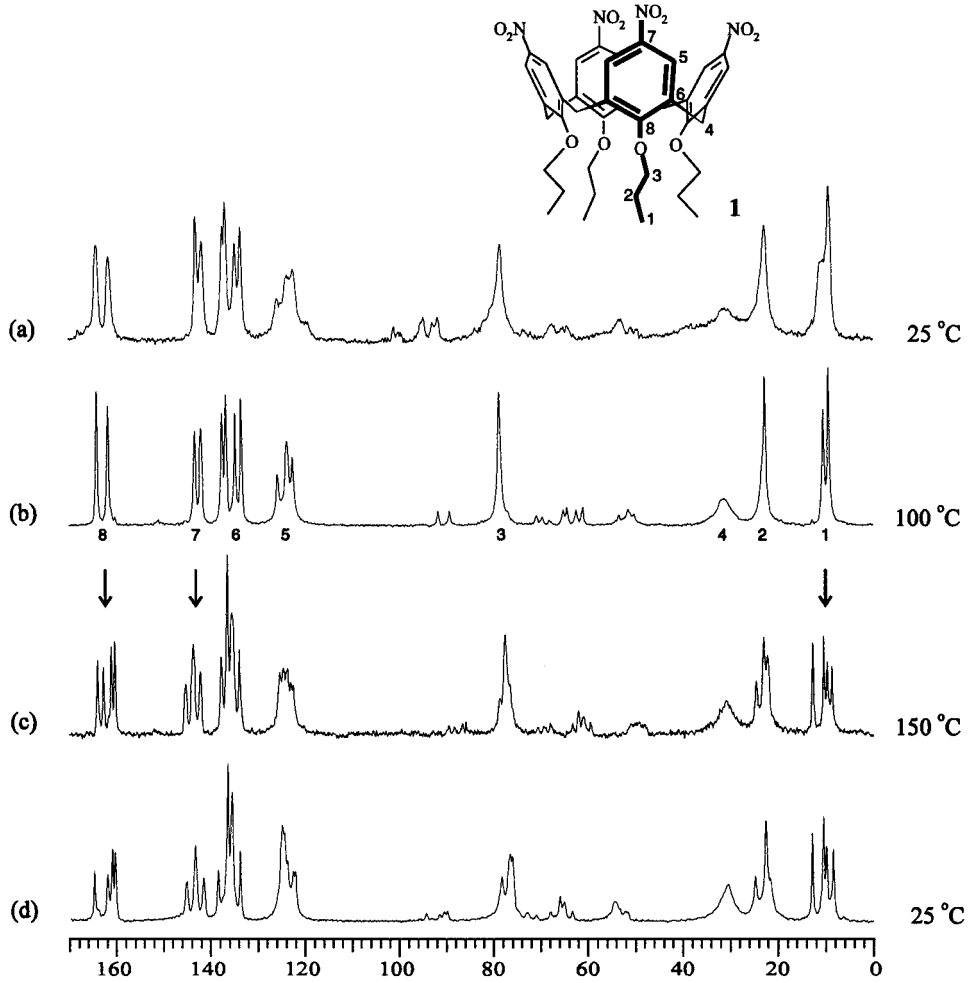

Figure 3. Temperature-dependent solid state ^{13}C NMR (CP-MAS) on microcrystalline tetranitrotetrapropoxycalix[4]arene **1**.

facets of the same crystal structure or by different crystal structures. To establish the origin of the friction signal, the pull-off force of the silicon nitride tip was measured for the two types of domains. It has been demonstrated in the literature that the pull-off forces[26,27] and the friction between a (modified) tip and the surface can reveal differences in the chemical composition of the surface.[28,29] The results of the force measurements, which were carried out under water in order to avoid capillary forces,[26] are plotted in Figure 5. The histograms in this figure show that the average pull-off force on domain type I ($F = 3.1 \pm 0.6$ nN) is ca. 2.4 times higher than that on domain type II ($F = 1.3 \pm 0.4$ nN). Such a large difference indicates that different functional groups are exposed at the surface of the two domains.[30]

In recent papers describing the use of chemically modified SFM tips[28,29] it was shown that, as a first approximation, the pull-off force correlates with the friction force. In our case, the observed difference in friction for different types of domains (I and II) can be attributed to the different functional groups at the film surface. However, the relative magnitude of the friction measured in the different domain types is inverted in water as compared to the situation in air. In water, solvent exclusion effects are responsible for the large pull-off forces observed with hydrophobic surfaces, whereas in air usually capillary forces dominate and consequently higher friction is observed for more hydrophilic surfaces.[29d] Furthermore, the difference in phase shift observed in the tapping mode phase image (Figure 4b) also indicates differences in adhesion forces and thus corresponds to exposure of different functional groups at the surfaces of type I and II domains.[25]

The friction of the two types of domains shows an unusual load dependence, as is depicted in Figure 6. In this figure, two friction force images of the same area are shown, obtained with different normal forces in air. The left image was captured with a normal force of ca. 225 nN, while the right image of the same area was acquired with a normal force of ca. 325 nN.

Although all type I domains have an identical appearance in SFM height images and in optical micrographs,

(26) (a) Weisenhorn, A. L.; Hansma, P. K.; Albrecht, T. R.; Quate, C. F. *Appl. Phys. Lett.* **1989**, *54*, 2651. (b) Weisenhorn, A. L.; Maivald, P.; Butt, H.-J.; Hansma, P. K. *Phys. Rev. B* **1992**, *45*, 11226.

(27) For adhesion measurements with silicon nitride tips see: Berger, C. E. H.; van der Werf, K. O.; Kooyman, R. P. H.; de Grooth, B. G.; Greve, J. *Langmuir* **1995**, *11*, 4188.

(28) (a) Frisbie, D.; Rozsnyai, L. F.; Noy, A.; Wrighton, M. S.; Lieber, C. M. *Science* **1994**, *265*, 2071. (b) Noy, A.; Frisbie, D.; Rozsnyai, L. F.; Wrighton, M. S.; Lieber, C. M. *J. Am. Chem. Soc.* **1995**, *117*, 7943. (c) Vezenov, D. V.; Noy, A.; Rozsnyai, L. F.; Lieber, C. M. *J. Am. Chem. Soc.* **1997**, *119*, 2006.

(29) (a) Thomas, R. C.; Tangyunyong, P.; Michalske, T. A.; Crooks, R. M. *J. Phys. Chem.* **1994**, *98*, 4493. (b) Akari, S.; Horn, D.; Keller, H.; Schrepp, W. *Adv. Mater.* **1995**, *7*, 549. (c) Green, J.-B. D.; McDermott, M. T.; Porter, M. D.; Siperko, L. M. *J. Phys. Chem.* **1995**, *99*, 10960. (d) Sinniah, S. K.; Steel, A. B.; Miller, C. J.; Reutt-Robey, J. E. *J. Am. Chem. Soc.* **1996**, *118*, 8925.

(30) Type I domains expose both nitro and propoxy groups (Figures 10 and 11), while optical microscopy suggests that the molecules in type II domains are lying on their sides. For type II domains in different orientations the observed complete extinction or transparency suggests a rotation perpendicular to the dipole axis. For the AFM force measurements the contact area between the tip and the sample surface has been assumed to be the same for both types of domains.

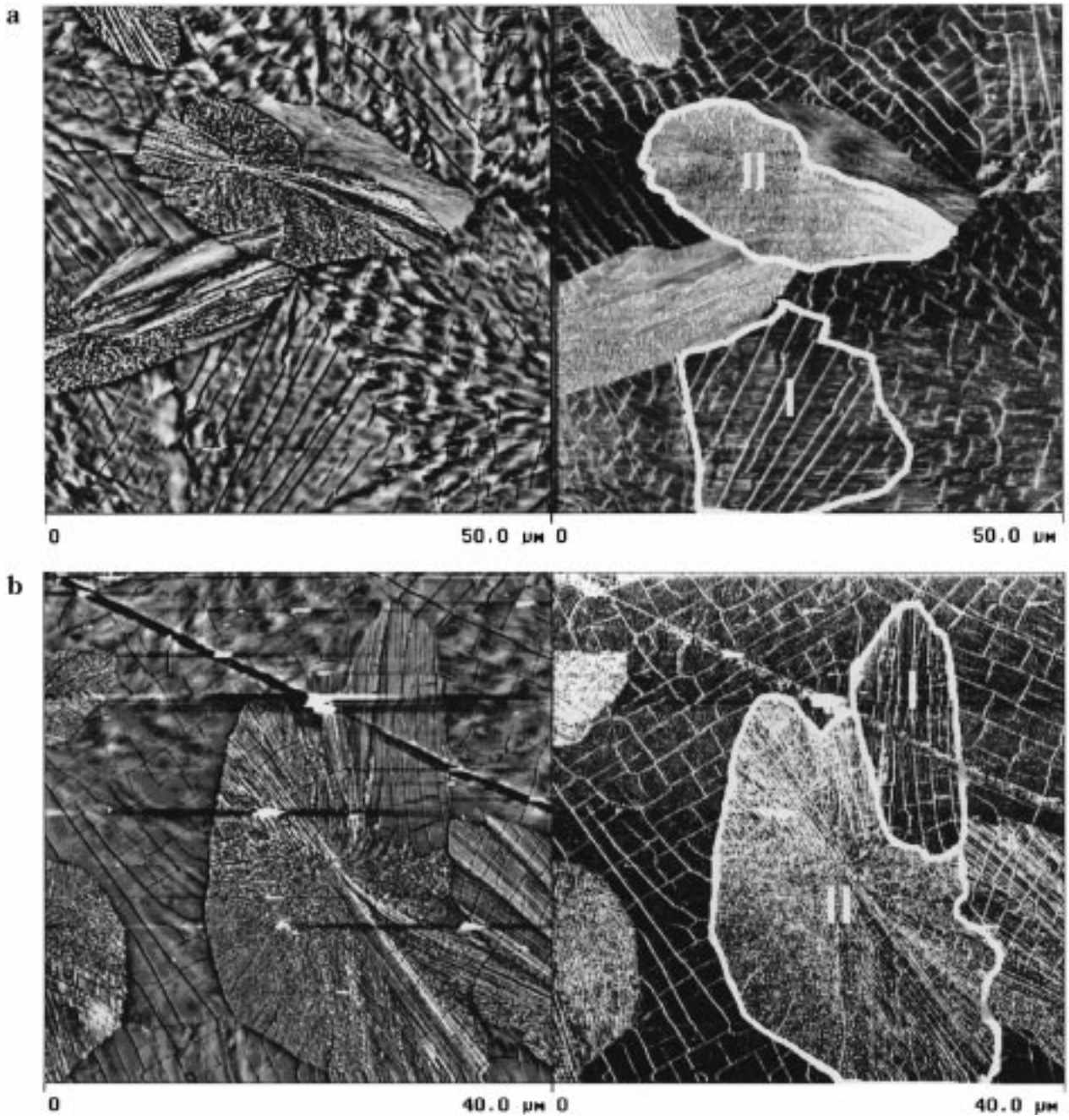

Figure 4. (a) Dual height (left, $z = 50$ nm) and friction force (right, $z = 0.5$ V) micrograph (contact mode) of an annealed film of **1**. (b) Tapping mode height (left, $z = 150$ nm) and phase image (right, $z = 75°$) of an annealed film of **1**.

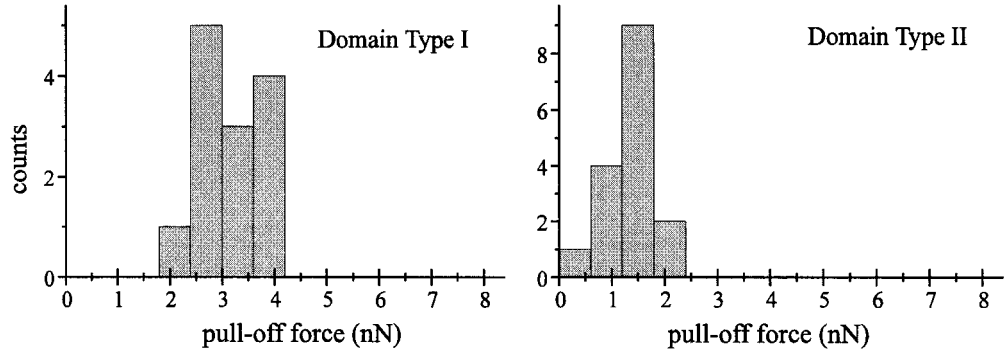

Figure 5. Pull-off forces between the silicon nitride tip and different types of domains of the films measured in water.

two domains of type I, which are marked as I**a** and I**b** in Figure 6, can be distinguished by *friction force microscopy*. The domains of type I**a** show a friction *similar* to that of domains I**b** at low forces, but at higher normal forces there is a *clear difference* (Figure 6). This difference in friction is not due to differences in functional groups exposed to

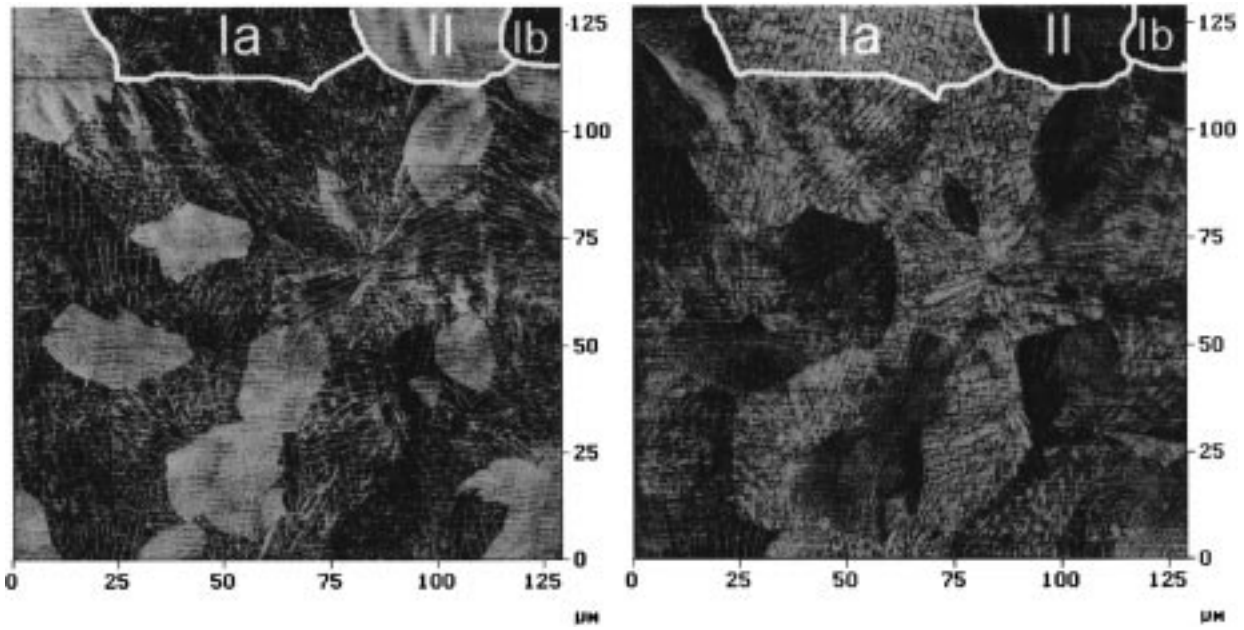

Figure 6. Friction force micrograph obtained at a normal force of ca. 225 nN (left), and ca. 325 nN (right) in air. Two different type I domains (Ia and Ib) and a type II domain are marked by white lines.

the surface, as is the case for type I and type II domains (vide supra), since the pull-off forces for domains of type I**a** and I**b** measured under water are identical. In addition, the appearance of the terrace-like morphology of both domains of type I is the same. Domains I**a** and I**b** do differ, however, in the orientation of the parallel cracks[31] observed in the optical and the SFM micrographs (compare Figures 1, 4, 6, and 8), with respect to the scanning direction. This is a clear indication that the frictional difference in type I domains correlates with the orientation of the surface crystal lattice (*friction anisotropy*). This relation between the macroscopic friction anisotropy and the structure at the molecular level was further investigated by high-resolution SFM (vide infra).

Inversion of Relative Friction. For normal forces below ca. 240 nN (Figure 6, left), the friction of the type I domains is *lower* than that of the type II domains, but for forces higher than 260 nN (Figure 6, right) type I**a** domains have a *higher* friction than type II domains.[32] The inversion in friction between type I**a** and type II domains was quantitatively evaluated by determining, at different normal forces, the friction forces of a large number of type I**a** and type II domains from the average of the friction value for each pixel.[33] Figure 7 gives the normalized friction values for the different domains as a function of the normal force. The plots show that the reversible transition of the friction contrast is located between 240 and 275 nN normal force values.[34]

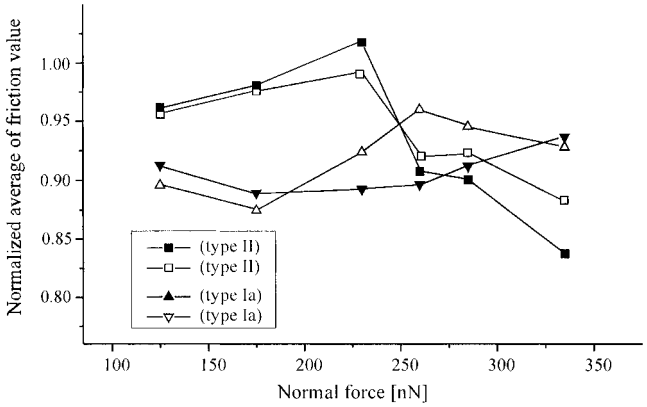

Figure 7. Normalized averages of friction value for different domains as a function of the normal force. The lines are included for clarity.

Molecular Packing. To determine the packing of the molecules and to prove the hypothesis that the regular spacing of the cracks in type I domains correlates with the underlying crystal structure, high-resolution SFM imaging in contact mode was performed. Unfortunately, it has been impossible to image a lattice structure with molecular resolution in type II domains until now. For type I domains it was possible to image the lattices of the surface crystal structure on the regular terraces such as those shown in Figure 8 (in height and friction images). These terraces have step heights of ca. 10 Å. This corresponds to the height of one molecule (9.2 Å based on molecular modeling, CPK models).

Two different surface lattices, which require the same area per molecule, can be observed in high-resolution SFM images (Table 1). One lattice has a rectangular symmetry (Figure 9, left) while the other possesses a pseudohexagonal packing (Figure 9b, right). These two structures probably represent two different facets of the same bulk crystal (vide infra). However, the coexistence of different polymorphic forms, e.g., as observed for PPTA by SFM,[35] cannot be excluded.

By X-ray crystallography an orthorhombic unit cell with lattice repeat units of $a = 23.94$ Å, $b = 33.01$ Å, and $c =$

(31) During cooling, the crystallized material may suffer from internal stress due to differences in the thermal expansion coefficient of the glass substrate and the annealed film of **1**, which leads to periodic cracks whose directions have a defined relation with the crystal lattice.

(32) Although more domains of type I**a**, I**b**, and II are visible, only three domains at the upper side are marked since a comparison of relative friction for domains that are not next to each other is unreliable because of the SFM plane-fitting procedure.

(33) Due to difficulties in measuring the friction force quantitatively in line scans (similar as in (a) Liu, Y.; Wu, T.; Evans, D. F. *Langmuir* **1994**, *10*, 2241. (b) Xiao, X.; Hu, J.; Charych, D. H.; Salmeron, M. *Langmuir* **1996**, *12*, 235), which were caused by the sample topology, an alternative approach was used.

(34) The inversion of friction contrast is indeed reversible. Damage to the sample surface was only observed once for a very sharp tip. For this probe, scanning at normal forces as low as ca. 50 nN led to a destruction of the sample surface.

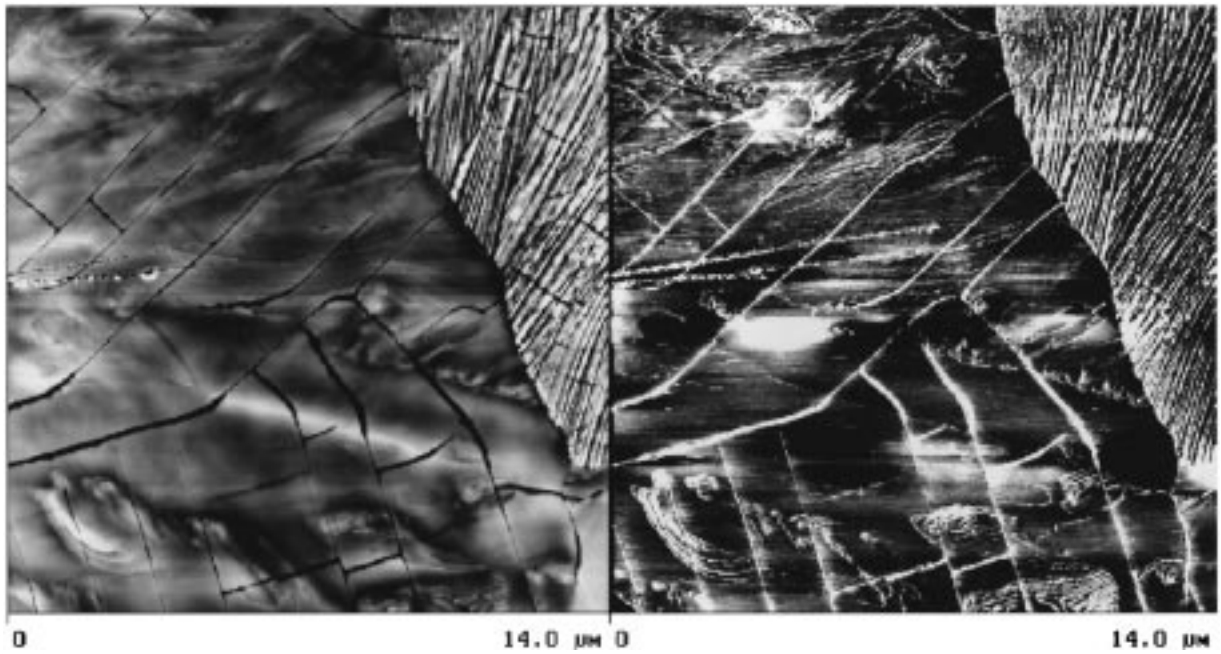

Figure 8. Dual height and friction force micrograph of type I and type II domains.

Table 1. Lattice Constants of Crystal Structures As Found by SFM in Type I Domains

lattice symmetry	lattice parameter (Å)	angle (deg)	area per molecule (Å^2)
hexagonal	$d = 11.6 \pm 0.3$	60 ± 2	116.5
rectangular	$x = 10.0 \pm 0.2$	90 ± 1	118.0
	$y = 11.8 \pm 0.2$		

20.59 Å was determined.[36] The *a* and *c* lattice distances of the X-ray structure match well with twice the corresponding values of the lattice parameters, as found by SFM for the rectangular symmetry (Table 1). Furthermore, the pattern observed by SFM matches perfectly with the number and orientation of the calix[4]arene molecules on the *ac* face ((010) facet) (Figure 10). It can be concluded that the SFM height image shows each of the molecules exposed at the crystal surface, but further details, such as the precise orientation of molecules or functional groups, are not resolved.

After examination of all facets of the single-crystal X-ray structure a pseudohexagonal packing of the calix[4]arene molecules was found in the (011) facet (Figure 11). This structure has lattice constants of 11.9 and 11.4 Å with an angle close to 60°, which is close to the hexagonal lattice constant of 11.6 ± 0.3 Å, as found by SFM (Table 1).[37,38] Other crystal facets could be excluded on the basis of the area per molecule requirements (Table 2). The (010) and (011) facets show areas per molecule that agree to within the experimental error with the SFM results.

Therefore it is likely that the hexagonal lattice as imaged by SFM represents a different facet of the *same* crystal structure. The repeat distance in the plane normal to the (011) facets was found by single-crystal crystallography to be 8.7 Å, whereas the repeat distance normal to the (010) facet was found to be 8.25 Å. Since the repeat distance *in the films* was determined to be 8.9 Å by X-ray diffraction (vide supra), the bulk crystal structure is probably the one with the (011) facet parallel to the surface. The coexistence of a second surface lattice, the (010) facet, can be attributed to partial surface relaxation resulting in epitaxial growth of the (010) facet on the (011) facet.[39]

The friction anisotropy observed for type I domains of the calixarene films (vide supra) can be attributed directly to the orientation of the lattice since in a large number of domains the orientation of the rectangular lattice was found to be parallel to the crack direction. The orientations of the molecules in *both* surface crystal structures are similar (compare Figures 10 and 11).[40] In both (010) and (011) facets, the orientation of the nitro groups and thus the orientation of the dipole moments of the molecules exposed to the surface are highly anisotropic. Therefore,

(35) (a) Snétivy, D.; Vancso, G. J.; Rutledge, G. C. *Macromolecules* **1992**, *25*, 7037. (b) Glomm, B. H.; Grob, M. C.; Neuenschwander, P.; Suter, U. W.; Snétivy, D.; Vancso, G. J. Polym. Commun. **1994**, 35, 878. (c) Rutledge, G. C.; Snétivy, D.; Vancso. G. J. Studies of high performance fibers by atomic force microscopy and molecular simulation. In *Atomic Force Microscopy/Scanning Tunneling Microscopy*; Cohen, S. H., et al., Eds.; Plenum Press: New York, 1994; p 251.

(36) The crystal structure is described in ref 7. Crystals were grown from chloroform/methanol in order to avoid inclusion of dichloromethane as observed earlier by Kelderman et al.: Monoclinic, *C*2/*c*, $a = 14.83$ Å, $b = 16.64$ Å, $c = 17.48$ Å. (Kelderman, E.; Derhaeg, L.; Verboom, W.; Engbersen, J. F. J.; Harkema, S.; Persoons, A.; Reinhoudt, D. N. *Supramol. Chem.* **1993**, *2*, 183.) These lattice distances differ considerably from the lattice distances found by SFM. This can be attributed to the presence of one dichloromethane molecule per calix[4]arene in the unit cell of the single crystal.

(37) In the determination of the hexagonal lattice constant, a difference was observed in the average lattice constant in different directions. For example: 11.5 and 11.7 ± 0.3 Å for one set of micrographs and 11.4 and 11.7 ± 0.3 Å for another set of micrographs, recorded on a different day. Since the difference between the two lattice constants is smaller than the standard deviation, we report an average value of 11.6 ± 0.3 Å, although there is an experimental indication that the structure as observed in SFM is not perfectly hexagonal, in accordance with the (011) facet of the single-crystal X-ray structure.

(38) A second hexagonal structure in accordance with the AFM results could be a modification of the *ac* face (010) in which one row of molecules is translated by half a molecule in the *a* direction ($^1/_4$a). However, this option is less probable due to the resulting steric hindrance of the neighboring calix[4]arene molecules in the *b* direction.

(39) The fact that the (010) facet is formed epitaxially on top of the (011) facet can be explained by the similarity of the lattice distances as found by SFM [20.0 Å × 23.6 Å (010) and 20.3 Å × 23.4 Å (011)] and single-crystal X-ray diffraction [20.6 Å × 23.9 Å (010) and 19.4 Å × 23.9 Å (011)].

(40) Although in the (011) facet the molecules are organized in a pseudohexagonal lattice, they are all oriented with the molecular dipole axis perpendicular to the *a* axis (similar to the (010) facet). Crystallographically, both facets possess rectangular symmetry, which results in the observed friction anisotropy.

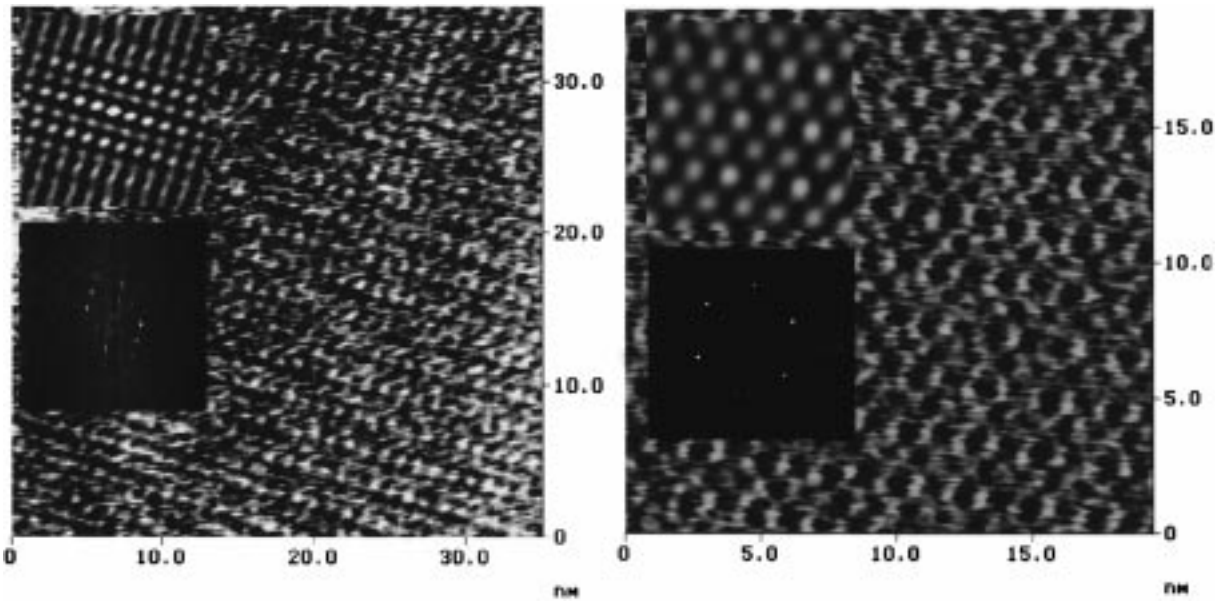

Figure 9. Rectangular crystal structure found in type I domain (left) and hexagonal crystal structure found in type I domain (right). SFM contact mode height images. Insets: autocovariance (top), 2-D Fourier transform (bottom).

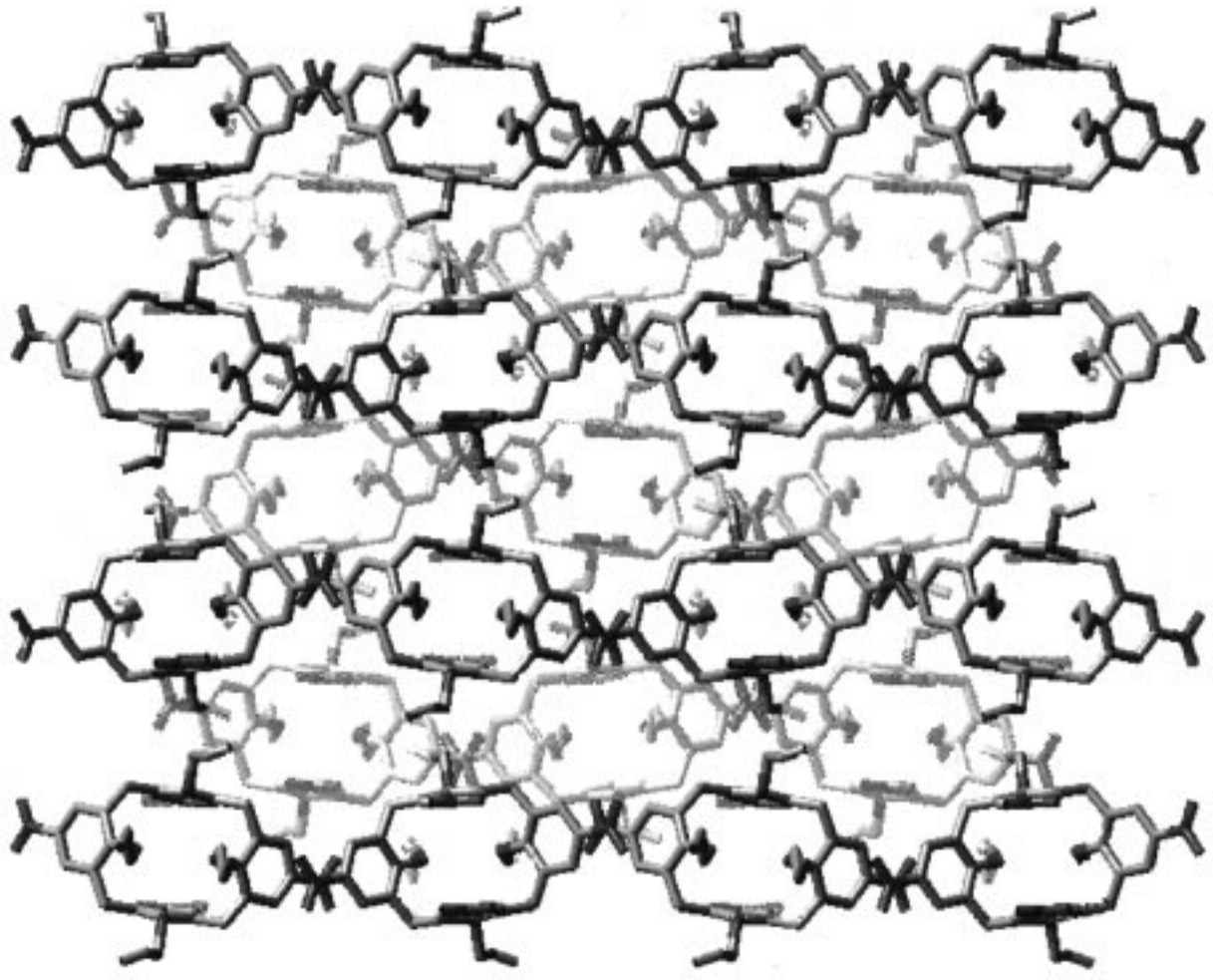

Figure 10. Depth contrast view of *ac* face ((010) facet) of the X-ray structure of tetranitrotetrapropoxycalix[4]arene (**1**).

the interaction of the SFM tip with the surface of the film is also expected to be anisotropic, and consequently, lattices with different orientation of the lattice (dipoles) with respect to the scanning direction result in different friction forces.

Conclusion

In tetranitrotetrapropoxycalix[4]arene (**1**) an irreversible phase transition from an amorphous to a crystalline phase in the region 130−140 °C was found by differential scanning calorimetry, optical microscopy, solid-state NMR,

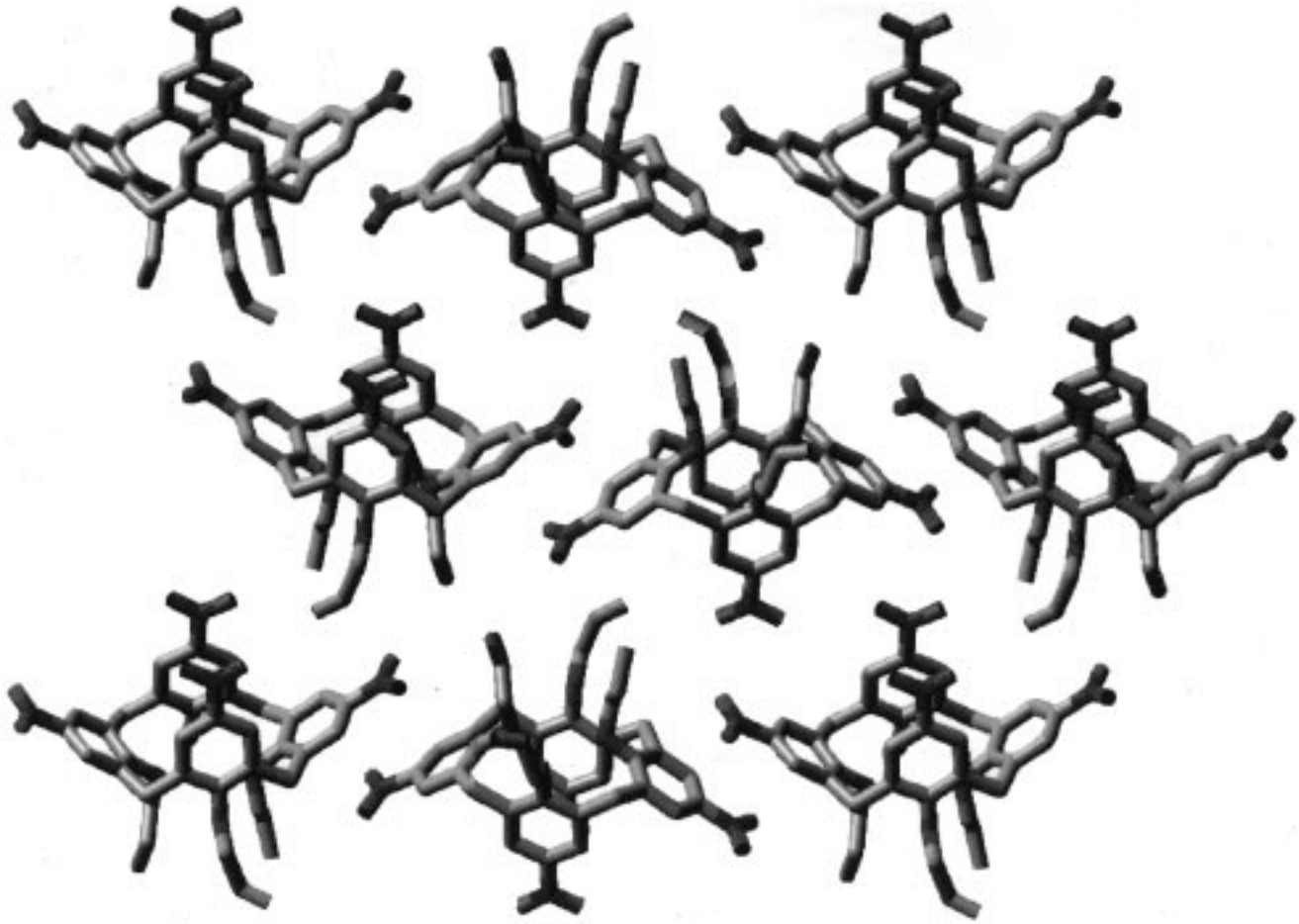

Figure 11. View of (011) facet of the X-ray structure of tetranitrotetrapropoxycalix[4]arene (**1**).

Table 2. Area Per Molecule for Different Crystal Facets of the Single-Crystal Structure of 1

crystal facet	area per molecule (Å^2)
(001)	174.4
(010)	123.2
(100)	197.6
(011)	116.4

and X-ray crystallography. The complex multidomain structure of annealed thin films of tetranitrotetrapropoxycalix[4]arene (**1**) was elucidated at the molecular level by using scanning force microscopy, optical microscopy, and X-ray diffraction. Two optically and morphologically different domains I and II were found, which exhibit a unique inversion of relative friction upon change of the load on the SFM tip. Furthermore, in domains of type I friction anisotropy was observed. This anisotropy could be shown to originate from different orientations of the surface crystal structure. High-resolution SFM revealed both a rectangular structure and a pseudohexagonal structure in type I domains. These lattices can be correlated to the (010) (rectangular lattice) and (011) (hexagonal) facets of the single-crystal structure of **1**. The coexistence of two lattices was attributed to partial surface relaxation.

Acknowledgment. We thank E. Klop for performing the powder X-ray diffraction, J. Boeijsma for performing the X-ray diffraction on thin films, and S. Picken for his help with the optical microscopy and valuable discussions. This investigation was financially supported by Akzo-Nobel, Electronic Products, Arnhem, and The Netherlands Foundation for Chemical Research (SON-NWO).

LA971198C